

Chemical Science

Accepted Manuscript

This article can be cited before page numbers have been issued, to do this please use: H. Land, P. Ceccaldi, L. Mészáros, M. Lorenzi, H. J. Redman, M. Senger, S. T. Stripp and G. Berggren, *Chem. Sci.*, 2019, DOI: 10.1039/C9SC03717A.



This is an Accepted Manuscript, which has been through the Royal Society of Chemistry peer review process and has been accepted for publication.

Accepted Manuscripts are published online shortly after acceptance, before technical editing, formatting and proof reading. Using this free service, authors can make their results available to the community, in citable form, before we publish the edited article. We will replace this Accepted Manuscript with the edited and formatted Advance Article as soon as it is available.

You can find more information about Accepted Manuscripts in the [Information for Authors](#).

Please note that technical editing may introduce minor changes to the text and/or graphics, which may alter content. The journal's standard [Terms & Conditions](#) and the [Ethical guidelines](#) still apply. In no event shall the Royal Society of Chemistry be held responsible for any errors or omissions in this Accepted Manuscript or any consequences arising from the use of any information it contains.

Discovery of Novel [FeFe]-Hydrogenases for Biocatalytic H₂-production

Henrik Land,^a Pierre Ceccaldi,^a Lívia S. Mészáros,^a Marco Lorenzi,^a Holly J. Redman,^a Moritz Senger,^b Sven T. Stripp^b and Gustav Berggren^{*a}

Received 00th January 20xx,
Accepted 00th January 20xx

DOI: 10.1039/x0xx00000x

www.rsc.org/

A new screening method for [FeFe]-hydrogenases is described, circumventing the need for specialized expression conditions as well as protein purification for initial characterization. [FeFe]-hydrogenases catalyze the formation and oxidation of molecular hydrogen at rates exceeding 10³ s⁻¹, making them highly promising for biotechnological applications. However, the discovery of novel [FeFe]-hydrogenases is slow due to their oxygen sensitivity and dependency on a structurally unique cofactor, complicating protein expression and purification. Consequently, only a very limited number have been characterized, hampering their implementation. With the purpose of increasing the throughput of [FeFe]-hydrogenase discovery, we have developed a screening method that allows for rapid identification of novel [FeFe]-hydrogenases as well as their characterization with regards to activity (activity assays and protein film electrochemistry) and spectroscopic properties (electron paramagnetic resonance and Fourier transform infrared spectroscopy). The method is based on *in vivo* artificial maturation of [FeFe]-hydrogenases in *Escherichia coli* and all procedures are performed on either whole cells or non-purified cell lysates, thereby circumventing extensive protein purification. The screening was applied on eight putative [FeFe]-hydrogenases originating from different structural sub-classes and resulted in the discovery of two new active [FeFe]-hydrogenases. The [FeFe]-hydrogenase from *Solobacterium moorei* shows high H₂-gas production activity, while the enzyme from *Thermoanaerobacter mathranii* represents a hitherto uncharacterized [FeFe]-hydrogenase sub-class. This latter enzyme is a putative sensory hydrogenase and our *in vivo* spectroscopy study reveals distinct differences compared to the well established H₂ producing HydA1 hydrogenase from *Chlamydomonas reinhardtii*.

Introduction

Molecular hydrogen (H₂) is broadly accepted as one of the most promising energy vectors to replace fossil fuels in a future sustainable society. With its superior gravimetric energy density (approximately three times higher than gasoline)¹ and clean combustion to H₂O, it is a good option for storing energy originating from renewable but intermittent sources like solar, wind and wave power. There are however drawbacks hampering the implementation of H₂ as a general energy carrier, such as the lack of sustainable production methods.² Currently, the industrial standard for producing H₂ is non-renewable steam methane reforming which produces CO₂ as a by-product. New methods for the production of H₂ are therefore needed, relying on catalysts based on cheap and abundant elements.

Biocatalysis has positioned itself as a major player in sustainable large-scale production of both fine- and bulk chemicals.^{3, 4} The

capacity of enzymes to catalyze chemical transformations with remarkable efficiency, specificity and selectivity make them highly relevant also in an energy context. Moreover, biocatalysts are attractive from a green chemistry point of view due to their ability to perform efficient catalysis at ambient temperatures in aqueous solution, without relying on noble metals. Hydrogenases are enzymes that catalyze the reversible reduction of protons to H₂.⁵ The most promising hydrogenase for biotechnological application is [FeFe]-hydrogenase due to its remarkable H₂-production activity with turnover frequencies as high as 9000 s⁻¹.⁶ Enzymes from this class of hydrogenases are primarily found in anaerobic bacteria and some green algae, and are dependent on a hexanuclear iron cofactor, commonly referred to as the H-cluster for catalysis.⁵ The H-cluster consists of a [4Fe-4S]-cluster coupled to a diiron complex, the [2Fe] subsite, via a bridging cysteine residue. The low valent metals of the [2Fe] subsite are coordinated by CO and CN⁻ ligands and bridged by an azapropanedithiolate ligand (–SCH₂NHCH₂S–, adt). The unique nature of the H-cluster in combination with its oxygen sensitivity results in difficulties when expressing [FeFe]-hydrogenases, as common and well-known expression hosts like *Escherichia coli* (*E. coli*) do not natively produce any [FeFe]-hydrogenases and therefore lack the [2Fe] subsite maturation machinery (HydEFG). Thus, standard over-expression techniques result in the synthesis of an inactive *apo*-enzyme, i.e. [FeFe]-hydrogenase harbouring only the active site [4Fe-4S]-

^a Molecular Biomimetics, Department of Chemistry – Ångström Laboratory, Uppsala University, Box 523, SE-75120, Uppsala, Sweden;

*Gustav.Berggren@kemi.uu.se

^b Institute of Experimental Physics, Experimental Molecular Biophysics, Freie Universität Berlin, Arnimallee 14, DE-14195, Berlin, Germany

Electronic Supplementary Information (ESI) available: Including experimental details and additional electrochemistry- and EPR data. See DOI: 10.1039/x0xx00000x



cluster but lacking the [2Fe] subsite. To some extent, this challenge can be overcome by utilizing specific *E. coli* strains, co-expressing the [FeFe]-hydrogenase specific maturases needed to synthesize the [2Fe] subsite and deliver it to the active site of the enzyme.^{7, 8} Alternatively, techniques have now been developed for the preparation of semi-synthetic hydrogenases, circumventing the need for the maturation machinery. The *apo*-enzyme can be anaerobically purified from *E. coli*, followed by artificial maturation of the *apo*-hydrogenase with a synthetic mimic of the [2Fe] subsite, $[\text{Fe}_2(\text{adt})(\text{CO})_4(\text{CN})_2]^{2-}$ ($[\text{2Fe}]^{\text{adt}}$), forming a fully active *holo*-enzyme.⁹⁻¹³ Still, extensive work is needed to obtain sufficient quantities of purified enzyme to perform artificial maturation and characterization. As a consequence, only a few [FeFe]-hydrogenases are currently characterized,¹¹⁻¹⁸ despite the diverse nature of this enzyme family.¹⁹⁻²³ All [FeFe]-hydrogenases feature the central H-domain, containing the aforementioned H-cluster. In addition, several sub-classes have been identified on genomic level, ranging from monomeric enzymes with one domain to multimeric enzymes with up to nine distinct domains. The influence of these additional domains on the activity and stability of the enzyme is still largely unknown. In order to establish the viability of [FeFe]-hydrogenase in a biotechnological context, e.g. as catalysts for H_2 -production, discovery of novel enzymes needs to become more effective to expand the toolbox of available [FeFe]-hydrogenases. Recently, we have shown that artificial maturation of the [FeFe]-hydrogenase from *Chlamydomonas reinhardtii* (*Cr*-HydA1) can be performed *in vivo* by supplying $[\text{2Fe}]^{\text{adt}}$ directly to living cells heterologously expressing the hydrogenase *apo*-enzyme. This results in *Cr*-HydA1 promoted H_2 -production in both *E. coli* as well as the cyanobacterium *Synechocystis* sp. 6803.^{24, 25} Moreover, we have reported how the cofactor of the resulting semi-synthetic enzyme can be monitored *in vivo* by electron paramagnetic resonance (EPR).²⁶ Herein we present how the combination of artificial maturation and biophysical characterization under *in vivo* conditions can be turned into a tool for efficient screening of novel [FeFe]-hydrogenases. The method is applicable to a range of *E. coli* expression and growth conditions, and allows for basic characterization without the need for time-consuming protein purification. We have also expanded the method by including

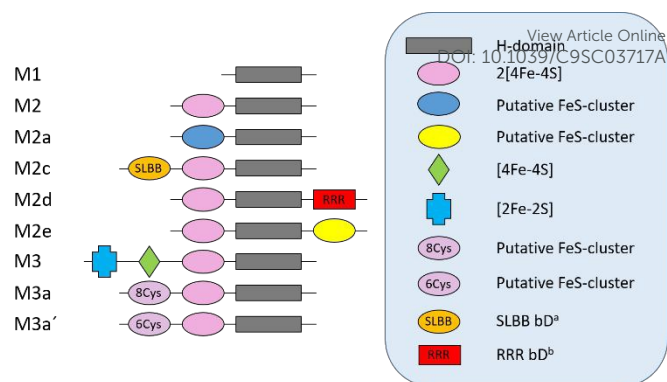


Figure 1. Schematic representation the various domains present in the eight sub-classes of putative [FeFe]-hydrogenases subject of this study (M2 and M3 enzymes). *C. reinhardtii* HydA1, representing a ninth additional sub-class (M1) was added as a positive control. ^a Soluble-ligand-binding β -grasp binding domain. ^b Rubredoxin-rubredoxin binding domain. The nomenclature was adapted from Meyer (2007)¹⁹ and Calusinska et. al. (2010)²⁰

whole-cell Fourier transform infrared (FTIR) spectroscopy²⁷ as well as protein film electrochemistry on non-purified cell lysates. To our knowledge, this is the first time the latter has been reported, and they both provide strong complementary additions to the presented method for discovery and characterization of novel [FeFe]-hydrogenases. More specifically, the screening allowed us to identify a representative enzyme of the hitherto uncharacterized M2e sub-class. This putative sensory hydrogenase was compared to the previously studied [FeFe]-hydrogenase from *Chlamydomonas reinhardtii* as well as a new example from the M2 sub-class.

Results and discussion

As a proof of concept, we have screened eight hitherto uncharacterized putative [FeFe]-hydrogenases, each originating from a different monomeric sub-class (Figure 1). These specific sub-classes were chosen for investigation based on earlier bioinformatic investigations (Figure 1), and the majority are so far completely uncharacterized.¹⁹⁻²³ The well-studied [FeFe]-hydrogenase from *C. reinhardtii* (*Cr*-HydA1) belonging to sub-class M1 (sub-class nomenclature is derived from Meyer²⁰ and Calusinska et. al.²¹) was included as a positive control as it has

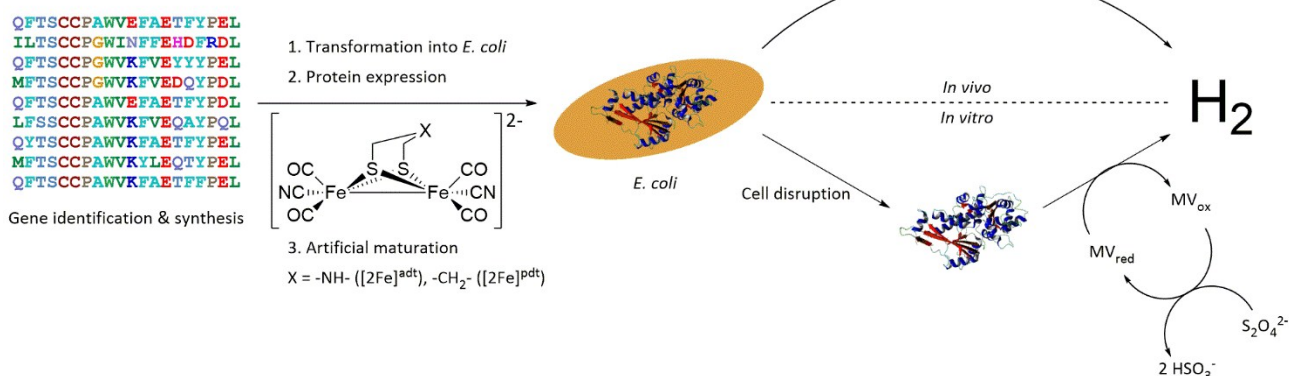


Figure 2. Representation of the workflow from gene identification to H_2 -production, either *in vivo* or *in vitro* activity assays. *C. reinhardtii* HydA1 is used as a representative 3D protein structure (PDB ID: 3LX4).



Table 1. Relative H₂-production activities of all screened putative [FeFe]-hydrogenases compared to *Cr*-HydA1. Every additional + represents an approximate 10-fold increase in activity. “-” no activity detected; “(+)” trace activity detected. See Table S2 for NCBI accession IDs for all screened [FeFe]-hydrogenases. DOI: 10.1039/C9SC03717A

[FeFe]-Hydrogenase sub-class	pET-11a(+)				pMAL-c4x			
	BL21(DE3)		BL21(DE3) ΔiscR		BL21(DE3)		BL21(DE3) ΔiscR	
	<i>In vivo</i>	<i>In vitro</i>	<i>In vivo</i>	<i>In vitro</i>	<i>In vivo</i>	<i>In vitro</i>	<i>In vivo</i>	<i>In vitro</i>
M1 (<i>Cr</i> -HydA1)	+++	+++	++	+++	+++	+++	+++	+++
M2 (<i>Sm</i>-HydA)	(+)	++	-	++	-	++	-	++
M2a	(+)	-	-	-	-	(+)	-	(+)
M2c	-	-	-	-	-	(+)	-	-
M2d	-	-	-	(+)	(+)	(+)	-	-
M2e (<i>Tam</i>-HydA)	-	+	-	-	-	(+)	-	-
M3	-	-	-	-	-	-	-	-
M3a	(+)	-	-	-	-	-	-	-
M3a'	-	-	-	-	-	(+)	-	-

previously been shown to work under the presented *in vivo* conditions.^{24, 26} M1 is the structurally simplest known [FeFe]-hydrogenase sub-class consisting only of the H-domain (Figure 1). Putative [FeFe]-hydrogenase encoding genes from each sub-class were identified by using the protein basic local alignment search tool (pBLAST)²⁸ with previously published [FeFe]-hydrogenase sequences as templates,^{17, 20, 21, 29} and one gene from each sub-class was arbitrarily chosen. Amino acid sequences of the putative [FeFe]-hydrogenases were analysed using the Protein Subcellular Localization Prediction Tool (PSORT),^{30, 31} and all enzymes except for one were predicted to be soluble. The enzyme from sub-class M3a' was predicted to be membrane bound with a relatively low probability. However, as the predicted transmembrane region includes an iron-sulfur (FeS) binding motif identical to the well-known F-clusters identified in several [FeFe]-hydrogenases, the gene was still included in the screening under the assumption that it is soluble. The genes were synthesized, codon-optimized for expression in *E. coli* and subsequently cloned into a pET-11a(+) vector by Genscript®.

A small-scale initial screen for H₂-production was performed by expressing the putative [FeFe]-hydrogenases in 200 mL cultures of *E. coli* cells. Following a standard aerobic over-expression protocol, the *apo*-hydrogenases were activated *in vivo* with addition of [2Fe]^{adt} to the growth medium under anaerobic conditions. *In vivo* H₂-production was examined and cells were thereafter subjected to lysis and the cell lysate was investigated for *in vitro* H₂-production. The *in vitro* assay utilized a previously published protocol using reduced methyl viologen as electron donor (Figure 2).³² The robustness of the artificial maturation method was probed using *Cr*-HydA1 in a range of expression conditions and cell media, and no limitations were found in this initial screening (Table S1). Still, for the purpose of enzyme screening, each gene was expressed using two different plasmid constructs. They were either cloned in pET-11a(+) with an N-terminal StrepII-tag or in pMAL-c4x with an N-terminal StrepII-tag and a C-terminal maltose binding protein fusion-tag. The latter was added to increase solubility of potentially insoluble proteins. Every construct was expressed in two different *E. coli* strains, a strain optimized for expression of FeS-cluster proteins

(BL21(DE3) ΔiscR), as well as standard BL21(DE3). Activities in this initial screen are presented in Table 1 as relative activities versus *Cr*-HydA1. The latter hydrogenase had the highest activity under these conditions, while many of the other putative [FeFe]-hydrogenases did not display any significant activity. Albeit these low activity hits are indicative of an active [FeFe] hydrogenase (trace activities indicated as (+) in Table 1), they were close to the H₂-detection limit of the gas chromatograph and were therefore omitted in the next stage. As all proteins show a high expression, at least when expressed in BL21(DE3) (Figure S1), the lack of activity is most likely attributable to low protein solubility (Figure S2). Indeed, the majority of the screened enzymes did show at least trace activity when fused with the maltose binding protein. Other factors might include misannotation of genes, incomplete incorporation of FeS-clusters or slow H-cluster formation. These latter factors are however less likely to influence the outcome of the screening as the motifs required for a gene to encode for an [FeFe]-hydrogenase are well defined¹⁹⁻²³ and the *E. coli* BL21(DE3) ΔiscR strain has in several cases been shown to successfully incorporate FeS-clusters in multi domain [FeFe]-hydrogenases^{11, 13, 33}. Also, slow formation of the H-cluster has so far only been shown in one specific dimeric [FeFe]-hydrogenase from *Desulfovibrio desulfuricans*.¹¹ Still, two new active hydrogenases were clearly identified, derived from *Solobacterium moorei* (*Sm*-HydA) and *Thermoanaerobacter mathranii* (*Tam*-HydA), respectively (indicated in bold in Table 1).

According to the sequence analysis the *Sm*-HydA enzyme belongs to sub-class M2 and it contains an N-terminal domain featuring two [4Fe-4S]-cluster binding motifs, in addition to the H-domain (Figure 1). *Sm*-HydA is homologous to the previously characterized [FeFe]-hydrogenase from *Megasphaera elsdenii*^{12, 34} (58 % amino acid sequence identity), which also belongs to sub-class M2. *Sm*-HydA shows a 5-10 fold lower activity compared to *Cr*-HydA1 in the *in vitro* H₂-production assay in all four screened conditions (Table 1).



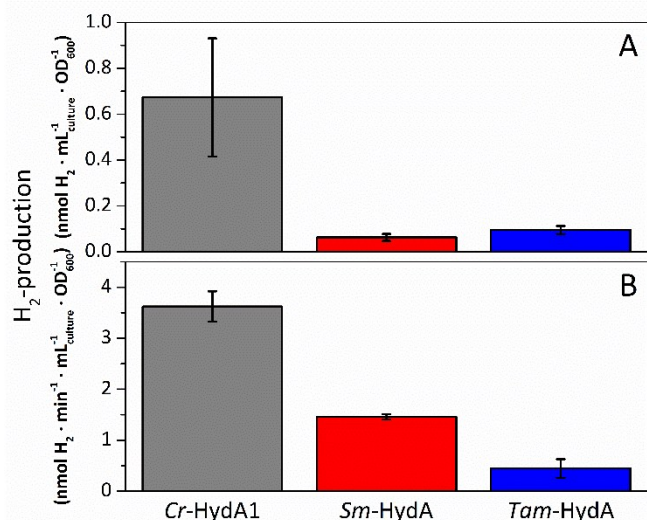


Figure 3. *In vivo* (A) and *in vitro* (B) H_2 -production activities of *Sm-HydA* and *Tam-HydA* compared to the positive control *Cr-HydA1*. *In vivo* H_2 -production was performed in glucose supplemented (0.4 %) M9 media. *In vitro* H_2 -production from cell lysates was performed in potassium phosphate buffer (100 mM, pH 6.8, 10 mM methyl viologen, 20 mM sodium dithionite and 1 % (v/v) Triton X-100).

Tam-HydA belongs to sub-class M2e and features the same domains as the aforementioned sub-class M2 hydrogenases. In addition, it also has an uncharacterized C-terminal domain with a conserved four-cysteine motif (Cx₂Cx₄Cx₁₆C), characteristic of an FeS-cluster binding site. Enzymes belonging to sub-class M2e are putative sensory hydrogenases, previously denoted as HydS.^{13, 35} On genome level *Tam-HydA* shows some similarity to a recently characterized sensory [FeFe]-hydrogenase from *Thermotoga maritima*.¹³ The latter enzyme has an additional C-terminal PAS (Per-Arnt-Sim) sensory domain commonly involved in signal transduction and belongs to sub-class M2f.²¹ As the PAS domain is lacking in *Tam-HydA* we will retain the HydA classification in the following text, as the sensory function remains to be verified. *Tam-HydA* cloned in pET-11a(+) and expressed in *E. coli* BL21(DE3) shows a 200-fold lower H_2 -production activity *in vitro* compared to *Cr-HydA1* (Table 1).

Sm-HydA and *Tam-HydA* were further investigated with regards to activity and spectroscopic properties. These follow-up studies were performed in *E. coli* BL21(DE3) with the genes cloned in pET-11a(+), as this condition provided activity for both enzymes in the initial screening. Thus, it allowed a comparison of the enzymes under the same conditions, and in the absence of bulky solubility tags.

A more detailed activity assessment with larger *E. coli* cultures was performed to quantify H_2 -production using the same assays as before (Figure 2). As shown in Figure 3A, *in vivo* H_2 -production was clearly observable under these conditions for both *Sm-HydA* and *Tam-HydA*, due to larger culture volumes and higher cell densities. The two enzymes display *in vivo* H_2 -production activities (0.062 ± 0.015 , *Sm-HydA*, and 0.095 ± 0.018 , *Tam-HydA*, $\text{nmol } H_2 \cdot \text{mL}_{\text{culture}}^{-1} \cdot \text{OD}_{600}^{-1}$) that are about eleven and seven times lower than *Cr-HydA1* (0.67 ± 0.26 $\text{nmol } H_2 \cdot \text{mL}_{\text{culture}}^{-1} \cdot \text{OD}_{600}^{-1}$), respectively. Conversely, the *in vitro* H_2 -production activity shows a different pattern (Figure 3B). *Cr-HydA1* is still the best H_2 -producer at 3.6 ± 0.30 $\text{nmol } H_2 \cdot \text{min}^{-1} \cdot \text{mL}_{\text{culture}}^{-1} \cdot \text{OD}_{600}^{-1}$ and similarly to the *in vivo* assays *Tam-HydA* has an eight times lower activity at 0.45 ± 0.18 $\text{nmol } H_2 \cdot \text{min}^{-1} \cdot \text{mL}_{\text{culture}}^{-1} \cdot \text{OD}_{600}^{-1}$. However, *Sm-HydA* has an activity of 1.5 ± 0.052 $\text{nmol } H_2 \cdot \text{min}^{-1} \cdot \text{mL}_{\text{culture}}^{-1} \cdot \text{OD}_{600}^{-1}$, i.e. approximately 40 % of the activity of *Cr-HydA1*. It remains unclear as to why the activity of *Sm-HydA* increases relative to the other enzymes following cell lysis. Sodium dithionite was added during *in vivo* activation in an attempt to simulate the reductive conditions of the *in vitro* assay but it showed no effect on the relative activities. This behaviour is therefore likely reflecting differences between the [FeFe]-hydrogenases in their affinity for the available electron donors in *E. coli* or the artificial electron donor methyl viologen.

Protein film electrochemistry was applied in order to gain further insight into the reactivity of the enzymes. The analysis was performed on non-purified cell lysates, following spontaneous adsorption of the enzymes onto carbon nanotube coated electrodes. No hydrogenase activity was detected for *Tam-HydA* under these conditions (Figure 4, grey trace), either due to insufficient binding to the electrode surface or low activity of *Tam-HydA* under these conditions. However, the activity of *Cr-HydA1* and *Sm-HydA* was readily detected and could be analysed and compared. Cyclic voltammetry traces of the two latter enzymes display clear catalytic waves corresponding to H_2 -production and oxidation (Figure 4 and Figure S3). Currents indicative of H_2 -production was detected both under 1 atm H_2 and 1 atm Ar, while the catalytic wave attributable to H_2 -oxidation is clearly absent under Ar. A sustained current was observed in chronoamperometry experiments performed under a H_2 atmosphere at an oxidizing potential, attributable to the oxidation of H_2 , and the *Sm-HydA* enzyme was stable on the electrode surface on the time-scale of the experiment (minutes) (Figure 5A, grey trace). H_2 partial pressure was varied between 1 and 0 atm by switching between H_2 - and Ar-bubbling (Figure 5B). As a result, the activity

Figure 4. Cyclic voltammogram of *Sm-HydA* containing cell lysate from *E. coli*. Analysis was performed either under H_2 (black) or Ar (red) at pH 6.0 and room temperature. The cyclic voltammogram recorded for *Tam-HydA* under H_2 shown in grey. Cycles start at -0.42 V vs SHE. Potential step 0.5 mV, scan rate 5 mV/s, electrode rotation speed 3 krpm.

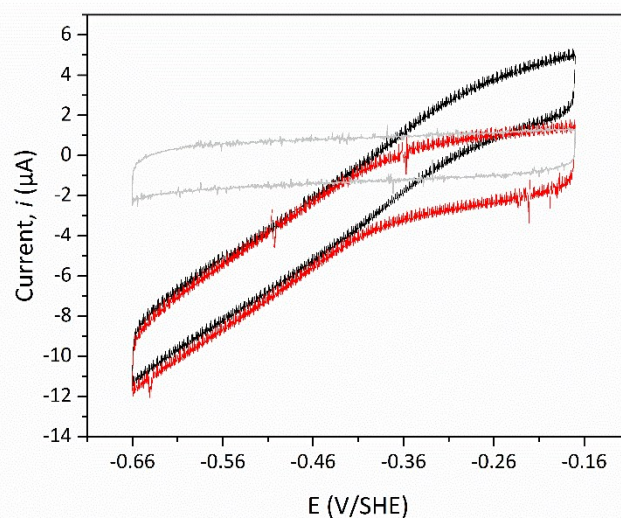


Figure 4. Cyclic voltammogram of *Sm-HydA* containing cell lysate from *E. coli*. Analysis was performed either under H_2 (black) or Ar (red) at pH 6.0 and room temperature. The cyclic voltammogram recorded for *Tam-HydA* under H_2 shown in grey. Cycles start at -0.42 V vs SHE. Potential step 0.5 mV, scan rate 5 mV/s, electrode rotation speed 3 krpm.



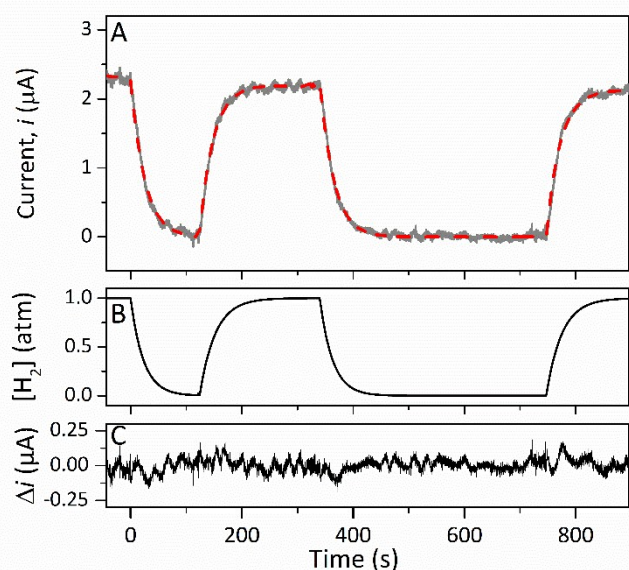


Figure 5. Chronoamperometry of *Sm-HydA* containing cell lysate from *E. coli* at a potential of -0.2 V/SHE. Current was measured over-time as a function of H_2 -pressure (A). H_2 -pressure was repeatedly varied between 0-1 atm (B), leading to a variation in H_2 -oxidation activity (A, grey trace). A Michaelis-Menten fit was performed (A, red dashed line) and returned a $K_M = 4$; given the experimental concentration range we conclude that $K_M(H_2)$ is >1 atm H_2 . The difference between the data and the fit was calculated (C). Solution at pH 7.0 and 25 °C, electrode rotation speed 3 krpm.

decreased and increased following the relative substrate availability (Figure 5A, grey trace). This trace was modelled with the Michaelis-Menten equation, where the substrate concentration is time-dependent (Figure 5A, red dashed line).³⁶ Here, K_M could only be determined as >1 atm H_2 , as the experimental setup did not allow use of pressures >1 atm. This shows that *Sm-HydA* has a lower affinity for H_2 than *Cr-HydA1*, for which a K_M of 0.57 ± 0.15 atm H_2 was determined (Figure S4), in agreement with the previously published value for the purified enzyme of 0.64 ± 0.05 atm H_2 .³⁶ The higher K_M for *Sm-HydA* suggests an improved bias towards H_2 -production over H_2 -oxidation, as compared to *Cr-HydA1*.

EPR spectroscopy is a sensitive spectroscopic technique for studying [FeFe]-hydrogenase, due to the characteristic signals of the H-cluster.^{5, 26} Thus we explored the possibility to utilize whole-cell X-band EPR spectroscopy in the presented screening to directly verify the presence of the enzyme. In order to facilitate the detection of the H-cluster, this study was performed using $[2Fe]^{adt}$ as well as an alternative $[2Fe]$ subsite mimic, $[2Fe]^{pdt}$ (pdt = propanedithiolate). The $[2Fe]^{pdt}$ cofactor mimic lacks the nitrogen bridgehead, resulting in a loss of catalytic rate and accumulation of an oxidized paramagnetic state (H_{ox}).^{9, 26, 38} EPR spectra recorded of whole-cell samples containing only the overproduced *apo*-hydrogenases (Figure 6 and Figure S5-S6, *apo-Sm-HydA* and *apo-Tam-HydA*) did not reveal any enzyme specific EPR signal(s). Similarly, *apo*-hydrogenase containing cells incubated with the $[2Fe]^{adt}$ complex did not reveal any well-defined new signal in the case of *Sm-HydA*, while maturation of *Tam-HydA* with $[2Fe]^{adt}$ resulted in a complex signal containing a mixture of different EPR active species (Figure S5). Contributions from an H_{ox} -like

state to the *Tam-HydA* spectrum is visible on the $g = 2.10$ feature, and additional signals at $g = 2.03$ and a broad $g = 1.90$ feature show similarities to signals previously observed for the *Thermotoga maritima* sensory [FeFe]-hydrogenase.¹³ Still, well-defined H-cluster signals were not readily apparent in either of the $[2Fe]^{adt}$ treated samples. Conversely, distinct H-cluster signals for both *Sm-HydA* and *Tam-HydA* could be detected in cells after incubation with the $[2Fe]^{pdt}$ cofactor. Whole cell samples of $[2Fe]^{pdt}$ -*Tam-HydA* displays a well-defined rhombic signal ($g_{zyx} = 2.10, 2.04, 2.00$) comparable to previously published data on identically treated *Cr-HydA1* (Figure 6, blue spectrum and Figure S6). It is therefore assigned to an H_{ox} -like state.²⁶ The signals for *Sm-HydA* were weak, preventing the identification of all g -values. Still, features at $g = 2.10$ and 2.04, attributable to an H_{ox} -like state was discernible also in $[2Fe]^{pdt}$ -*Sm-HydA* containing cells (Figure 6, red spectrum and inset, and Figure S6). Considering the intense EPR signal observed for $[2Fe]^{pdt}$ -*Tam-HydA* and the high expression level of *apo-Sm-HydA* (Figure S1), the weak EPR-signal observed for the latter enzyme is most likely due to low solubility of the overproduced protein (Figure S2), ineffective FeS-cluster incorporation or incomplete H-cluster assembly. Alternatively, it could be due to

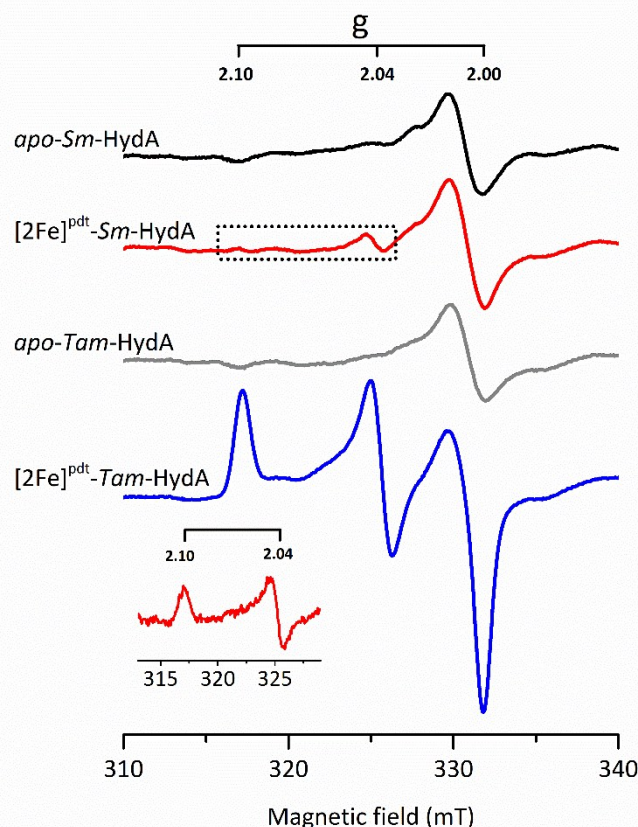


Figure 6. *In vivo* H-cluster assembly in *E. coli* monitored using X-band EPR spectroscopy. A rhombic EPR signal characteristic of the H_{ox} state is clearly observable in $[2Fe]^{pdt}$ -*Tam-HydA* ($g = 2.10; 2.04; 2.00$); two of these peaks are also apparent in $[2Fe]^{pdt}$ -*Sm-HydA* following subtraction of the cell background signals. Samples were collected from cells incubated in the absence (*apo-Sm-HydA* and *apo-Tam-HydA*) and presence of $[2Fe]^{pdt}$. Inset: $[2Fe]^{pdt}$ -*Sm-HydA* spectrum corrected for contribution from the cells by subtracting the *apo-Sm-HydA* signal. EPR experimental conditions: $T = 10$ K, $P = 1$ mW, $\nu = 9.28$ GHz.



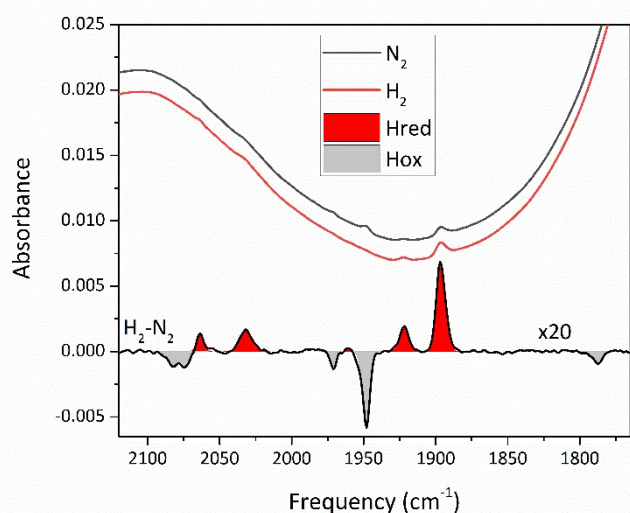


Figure 7. *In situ* ATR FTIR spectra of *Tam*-HydA containing *E. coli* cells activated with $[2\text{Fe}]^{\text{adt}}$. Absolute spectra under N_2 (black) and H_2 (red) are shown above a H_2 - N_2 difference spectrum (magnified 20x). Note the presence of H_{red} (e.g. the reporter peak at 1896 cm^{-1}), even under N_2 .

Table 2. Band positions of FTIR spectra in Figure 7.

Redox state	Cofactor ligand				
	CN^-	CN^-	CO	CO	CO
$\text{H}_{\text{ox}} (\text{cm}^{-1})$	2082	2074	1971	1948	1788
$\text{H}_{\text{red}} (\text{cm}^{-1})$	2063	2032	1961	1921	1896

a thermodynamic preference towards an EPR silent state. Nevertheless, EPR spectroscopy of $[2\text{Fe}]^{\text{adt}}$ treated cells verified the successful assembly of a semi-synthetic H-cluster in both enzymes.

To circumvent the limitations of EPR spectroscopy in detection of all catalytic states, we also employed whole-cell FTIR spectroscopy. The absorption bands of the H-cluster CN^- and CO ligands are typically exploited to track changes in cofactor geometry as well as in redox- and protonation states.⁵ For *Sm*-HydA, no cofactor ligand band signal could be detected, further indicating its low concentration in the *E. coli* cells. Figure 7 reports on the absorption spectrum of *E. coli* cells containing *Tam*-HydA activated with $[2\text{Fe}]^{\text{adt}}$ recorded by *in situ* attenuated total reflectance (ATR) FTIR spectroscopy in the CN^- and CO ligand frequency regime. The absolute spectra were recorded at pH 8 under N_2 - and H_2 -atmosphere and the main CO bands of the cofactor were clearly detectable. As prepared, the enzyme adopted a redox state with low frequency CO bands that was converted into a species with up-shifted CO bands upon extensive purging with N_2 . In the presence of H_2 , the original signature was immediately restored. The corresponding H_2 - N_2 difference spectrum (magnified 20-fold) allowed separation of two redox states associated with the different gas atmospheres (band positions in Table 2). In accordance with earlier studies on various $[\text{FeFe}]$ -hydrogenases, we assign positive bands to the reduced state H_{red} (red area) and negative bands to H_{ox} (grey area).^{13, 39-41} As can be seen in Figure 7, the two CN^- bands attributed to H_{ox} (2082 and 2074 cm^{-1}) are partially overlapping. Also, one of the CO bands assigned to H_{red} (1961 cm^{-1}) is barely

visible due to the close proximity of nearby CO bands belonging to H_{ox} (1971 and 1948 cm^{-1}). The observed formation of H_{red} in the presence of H_2 provides spectroscopic support for the capacity of *Tam*-HydA to perform H_2 oxidation. In addition, the slow and incomplete formation of H_{ox} under N_2 suggests inferior H_2 release activity. This is accompanied with an unusual persistence of H_{red} that was not observed with *E. coli* cells containing *Cr*-HydA1 (Figure S7), suggestive of distinct differences in the reactivity of the enzymes under *in vivo* conditions. Finally, our data also verifies that the whole-cell screening method is compatible with ATR-FTIR spectroscopy, providing a strong complement to the EPR spectroscopy.

Conclusions

Herein we present a straightforward method for rapid screening and basic characterization of novel $[\text{FeFe}]$ -hydrogenases, compatible with a range of *E. coli* expression conditions. The method is based on *in vivo* artificial maturation of overproduced *apo*- $[\text{FeFe}]$ -hydrogenase with synthetic cofactors and verification of hydrogenase activity through standard *in vitro* and/or *in vivo* activity assays. As presented herein, these enzymatic assays can also be supported by protein film electrochemistry while still avoiding any protein purification. We have also shown that whole-cell EPR and FTIR spectroscopy can be readily employed to complement the activity measurements and verify the successful expression also of apparent low activity $[\text{FeFe}]$ -hydrogenases, as exemplified by *Tam*-HydA. Despite low temperature induction and the use of solubility fusion protein constructs, the solubility of the proteins remains a significant challenge. This underscores the need to screen several enzymes to obtain hits suitable for purification and more detailed studies. Still, one of the main advantages of the presented method is that protein expression can be performed without specialized cells or conditions. Additionally, all analysis is carried out on whole cells or non-purified cell lysates, eliminating the need for extensive protein purification. This first proof of concept screening included putative $[\text{FeFe}]$ -hydrogenase genes from eight different structural sub-classes, and resulted in the discovery of two previously uncharacterized $[\text{FeFe}]$ -hydrogenases. On a methodology level, the activation of M2 (*Sm*-HydA) and M2e (*Tam*-HydA) enzymes under these assay conditions underscore that the method is capable of detecting also complex multi-domain hydrogenases with several FeS-clusters. Thus, the presented method can be expected to facilitate the discovery of novel $[\text{FeFe}]$ -hydrogenases, paving the way for understanding their complex chemistry and increasing the toolbox of available biocatalysts applicable in a future H_2 -society. Both *Sm*-HydA and *Tam*-HydA show distinctively different features as compared to *Cr*-HydA1. *Sm*-HydA displays high activity based on activity assays and protein film electrochemistry while spectroscopic data indicates a low concentration of the enzyme. In combination, these results suggest that *Sm*-HydA has a high specific activity, warranting further investigation. *Tam*-HydA, on the other hand, is readily detectable by EPR and FTIR spectroscopy, underscoring that the enzyme expresses well and is readily



matured under these conditions. Despite the high intracellular concentration, the enzyme displayed very low H₂-evolution activities. Moreover, the whole-cell FTIR spectroscopy study of *Tam*-HydA revealed an unexpected stability of H_{red} over H_{ox}. These observations support the notion that the latter enzyme indeed serves a sensory rather than catalytic function, as previously proposed for enzymes from sub-class M2e. As *Tam*-HydA is the first reported example of this sub-class, it provides an entry point into studying the reactivity and biological function of this hitherto unstudied type of [FeFe]-hydrogenase.

Conflicts of interest

There are no conflicts to declare.

Acknowledgements

The ERC (StG contract no. 714102) and the Swedish Research Council, VR (contract no. 621-2014-5670) as well as the German Research Foundation (DFG) through the priority program 1927 to STS are gratefully acknowledged for funding.

Notes and references

- M. B. Ley, L. H. Jepsen, Y.-S. Lee, Y. W. Cho, J. M. Bellosta von Colbe, M. Dornheim, M. Rokni, J. O. Jensen, M. Sloth, Y. Filinchuk, J. E. Jørgensen, F. Besenbacher and T. R. Jensen, *Mater. Today*, 2014, **17**, 122-128.
- I. Dincer and C. Acar, *Int. J. Hydrogen Energ.*, 2015, **40**, 11094-11111.
- U. T. Bornscheuer, G. W. Huisman, R. J. Kazlauskas, S. Lutz, J. C. Moore and K. Robins, *Nature*, 2012, **485**, 185-194.
- U. T. Bornscheuer, *Phil. Trans. R. Soc. A*, 2018, **376**, 20170063.
- W. Lubitz, H. Ogata, O. Rüdiger and E. Reijerse, *Chem. Rev.*, 2014, **114**, 4081-4148.
- R. Cammack, *Nature*, 1999, **397**, 214-215.
- J. M. Kuchenreuther, C. S. Grady-Smith, A. S. Bingham, S. J. George, S. P. Cramer and J. R. Swartz, *PLoS ONE*, 2010, **5**, e15491.
- P. W. King, M. C. Posewitz, M. L. Ghirardi and M. Seibert, *The Journal of Bacteriology*, 2006, **188**, 2163-2172.
- G. Berggren, A. Adamska, C. Lambert, T. R. Simmons, J. Esselborn, M. Atta, S. Gambarelli, J. M. Mouesca, E. Reijerse, W. Lubitz, T. Happe, V. Artero and M. Fontecave, *Nature*, 2013, **499**, 66-69.
- J. Esselborn, C. Lambert, A. Adamska-Venkatesh, T. Simmons, G. Berggren, J. Noth, J. Siebel, A. Hemschemeier, V. Artero, E. Reijerse, M. Fontecave, W. Lubitz and T. Happe, *Nat. Chem. Biol.*, 2013, **9**, 607-609.
- J. A. Birrell, K. Wrede, K. Pawlak, P. Rodriguez-Maciá, O. Rüdiger, E. J. Reijerse and W. Lubitz, *Isr. J. Chem.*, 2016, **56**, 852-863.
- G. Caserta, A. Adamska-Venkatesh, L. Pecqueur, M. Atta, V. Artero, S. Roy, E. Reijerse, W. Lubitz and M. Fontecave, *Biochim. Biophys. Acta, Bioenerg.*, 2016, **1857**, 1734-1740.
- N. Chongdar, J. A. Birrell, K. Pawlak, C. Sommer, E. J. Reijerse, O. Rüdiger, W. Lubitz and H. Ogata, *J. Am. Chem. Soc.*, 2018, **140**, 1057-1068.
- J.-S. Chen and L. E. Mortenson, *Biochim. Biophys. Acta, Protein Struct.*, 1974, **371**, 283-298. DOI: 10.1039/C9SC03717A
- C. Kamp, A. Silakov, M. Winkler, E. J. Reijerse, W. Lubitz and T. Happe, *Biochim. Biophys. Acta, Bioenerg.*, 2008, **1777**, 410-416.
- G. J. Schut and M. W. Adams, *J. Bacteriol.*, 2009, **191**, 4451-4457.
- S. Morra, M. Arizzi, F. Valetti and G. Gilardi, *Biochemistry*, 2016, **55**, 5897-5900.
- V. Engelbrecht, P. Rodriguez-Macia, J. Esselborn, A. Sawyer, A. Hemschemeier, O. Rüdiger, W. Lubitz, M. Winkler and T. Happe, *Biochim. Biophys. Acta, Bioenerg.*, 2017, **1858**, 771-778.
- P. M. Vignais, B. Billoud and J. Meyer, *FEMS Microbiol. Rev.*, 2001, **25**, 455-501.
- J. Meyer, *Cell. Mol. Life Sci.*, 2007, **64**, 1063-1084.
- M. Calusinska, T. Happe, B. Joris and A. Wilimotte, *Microbiology*, 2010, **156**, 1575-1588.
- J. W. Peters, G. J. Schut, E. S. Boyd, D. W. Mulder, E. M. Shepard, J. B. Broderick, P. W. King and M. W. W. Adams, *Biochim. Biophys. Acta, Mol. Cell Res.*, 2015, **1853**, 1350-1369.
- C. Greening, A. Biswas, C. R. Carere, C. J. Jackson, M. C. Taylor, M. B. Stott, G. M. Cook and S. E. Morales, *Isme J.*, 2016, **10**, 761-777.
- N. Khanna, C. Esmieu, L. S. Mészáros, P. Lindblad and G. Berggren, *Energ. Environ. Sci.*, 2017, **10**, 1563-1567.
- A. Wegelius, N. Khanna, C. Esmieu, G. D. Barone, F. Pinto, P. Tamagnini, G. Berggren and P. Lindblad, *Energ. Environ. Sci.*, 2018, **11**, 3163-3167.
- L. S. Mészáros, B. Németh, C. Esmieu, P. Ceccaldi and G. Berggren, *Angew. Chem. Int. Ed.*, 2018, **57**, 2596-2599.
- M. Horch, L. Lauterbach, M. Saggi, P. Hildebrandt, F. Lenzian, R. Bittl, O. Lenz and I. Zebger, *Angew. Chem. Int. Ed.*, 2010, **49**, 8026-8029.
- S. F. Altschul, W. Gish, W. Miller, E. W. Myers and D. J. Lipman, *J. Mol. Biol.*, 1990, **215**, 403-410.
- M. Atta and J. Meyer, *Biochim. Biophys. Acta, Protein Struct. Mol. Enzymol.*, 2000, **1476**, 368-371.
- K. Nakai and M. Kanehisa, *Proteins*, 1991, **11**, 95-110.
- K. Nakai and M. Kanehisa, *Genomics*, 1992, **14**, 897-911.
- H. D. Peck and H. Gest, *J. Bacteriol.*, 1956, **71**, 70-80.
- J. Esselborn, N. Muraki, K. Klein, V. Engelbrecht, N. Metzler-Nolte, U. P. Apfel, E. Hofmann, G. Kurisu and T. Happe, *Chemical Science*, 2016, **7**, 959-968.
- C. Van Dijk, S. G. Mayhew, H. J. Grande and C. Veeger, *Eur. J. Biochem.*, 1979, **102**, 317-330.
- Y. Zheng, J. Kahnt, I. H. Kwon, R. I. Mackie and R. K. Thauer, *J. Bacteriol.*, 2014, **196**, 3840-3852.
- V. Fourmond, C. Baffert, K. Sybirna, S. Dementin, A. Abou-Hamdan, I. Meynial-Salles, P. Soucaille, H. Bottin and C. Léger, *Chem. Commun.*, 2013, **49**, 6840-6842.
- P. Ceccaldi, K. Schuchmann, V. Müller and S. J. Elliott, *Energ. Environ. Sci.*, 2017, **10**, 503-508.
- A. Adamska-Venkatesh, D. Krawietz, J. Siebel, K. Weber, T. Happe, E. Reijerse and W. Lubitz, *J. Am. Chem. Soc.*, 2014, **136**, 11339-11346.
- W. Roseboom, A. L. De Lacey, V. M. Fernandez, E. C. Hatchikian and S. P. J. Albracht, *J. Biol. Inorg. Chem.*, 2006, **11**, 102-118.
- C. Sommer, A. Adamska-Venkatesh, K. Pawlak, J. A. Birrell,



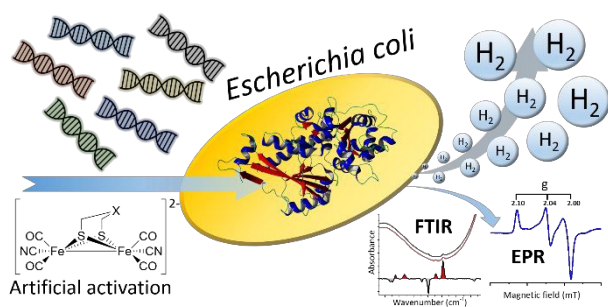
ARTICLE

Journal Name

- O. Rüdiger, E. J. Reijerse and W. Lubitz, *J. Am. Chem. Soc.*, 2017, **139**, 1440-1443.
41. S. Mebs, M. Senger, J. Duan, F. Wittkamp, U.-P. Apfel, T. Happe, M. Winkler, S. T. Stripp and M. Haumann, *J. Am. Chem. Soc.*, 2017, **139**, 12157-12160.

View Article Online
DOI: 10.1039/C9SC03717A





A semi-synthetic screening method for mining the biodiversity of [FeFe]-hydrogenases, expanding the toolbox for biocatalytic H₂-gas production

